Geomagnetism and Aeronomy, Vol. 42, No. 6, 2002, pp. 755–762. Translated from Geomagnetizm i Aeronomiya, Vol. 42, No. 6, 2002, pp. 790–797.

Registration of Ionospheric Responses to Shock Acoustic Waves Generated by Carrier Rocket Launches

E. L. Afraimovich, N. P. Perevalova, and A. V. Plotnikov

Institute of Solar–Terrestrial Physics, P.O. Box 4026, Irkutsk, 664033 Russia

Received October 30, 2001

Abstract—Possibilities of using the GPS and Transit satellite radionavigational systems (SRNS) for determining parameters of shock acoustic waves (SAW) generated during carrier rocket launches have been investigated. It has been indicated that the ionospheric response to SAW has a character of wave disturbances with periods of 250–300 s. Registration of these disturbances with a widely branched system of GPS receivers and their processing using the methods developed by us have made it possible to determine the main SAW characteristics: the wavevector azimuth and elevation angles, the horizontal components and magnitude of the phase velocity, and coordinates of a SAW source and the time of its activation. The above parameters calculated for 18 launches of the Proton and Soyuz carrier rockets from the Baikonur cosmodrome in 1998–2000 are presented. Model calculations have shown that data of Transit SRNS do not allow one to reliably detect a SAW response and to determine its parameters.

1. INTRODUCTION

Studying ionospheric disturbances that originate during launches of powerful vehicles, including spacecraft launch vehicles (LV) is of scientific interest, since we can consider such launches as active experiments in the Earth's atmosphere and use them to solve a number of problems of ionospheric physics and radiowave propagation. These studies are also of applied significance, since they allow us to substantiate reliable signal indications of technogenic effects (including unauthorized), necessary for constructing an effective global radiophysical system for detecting and localizing these effects.

By the present, a few types of disturbances caused by an active flight have been described [Karlov *et al.*, 1980]. The first type of the disturbance is generated during the interaction between an oncoming air flow and a rocket plume. This disturbance may have a space scale of about 10 km and directly joins a rocket airframe. The second type of the disturbance is characterized by a significant drop of the electron density N_e at altitudes of the F_2 layer, caused by the violation of the photochemical equilibrium of ionized particles due to the ejection of rocket exhausts into the ionosphere. The third type of the disturbance is related to SAW generated during a rocket launch. SAW generate in the Earth's atmosphere a wide spectrum of acoustic gravity waves (AGW) propagating over large distances and involving (via collisions) the charged component of the ionosphere into the wave motion.

Variations in electron density caused by a LV launch are recorded by different radiophysical methods. Traditional methods for detecting ionospheric disturbance include vertical and oblique incidence radiosounding of the ionosphere (ionosondes), measurements of a Doppler frequency shift during the vertical and oblique incidence radiosounding in the SW range, measurements of a Faraday rotation of the polarization plane of geostationary satellite signals, and incoherent scatter radars. The main drawback of the above methods during diagnosing short-time technogenic effects, including carrier rocket launches, is low resolution in time and space. The sensitivity of these methods allows us to detect and study large-scale effects, such as an expected drop of N_e in the F_2 layer, and, in a number of cases, to rather reliably detect wave ionospheric disturbances (WID) generated by a shock wave. Substantial difficulties arise, however, in determining the major WID parameters, the amplitude, phase, period, phase and group velocities, angular characteristics of a wavevector, and the region of formation. This explains the lack of complete and trustworthy data on WID characteristics despite the long-term investigations in this field.

Presently, the substantial progress is observed in the development of methods for monitoring processes in the Earth's atmosphere based on using SRNS. Using two-frequency receivers of such systems, one can realize high-accuracy measurements of the line of sight phase delay between a ground-based receiver and satellite transmitters simultaneously at two coherently coupled frequencies virtually at any time and at any point of the globe. Presently, these data, recalculated into a total electron content (TEC), are widely used for studying the regular ionosphere and natural and technogenic disturbances.

As a rule, the time resolution of measurements is very high for navigational systems. It varies from 1 s (Transit SRNS) to not more than 30 s (SRNS GPS) and allows one to study ionospheric disturbances in the

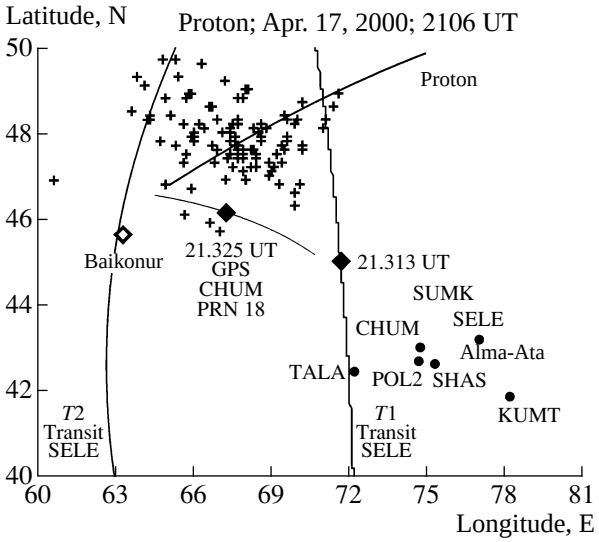

Fig. 1. Geometry of the experiments during launches of the Proton carrier rockets from the Baikonur cosmodrome in 2000. The sign ◇ (rhomb) indicates location of the launch site. Thick line approximately corresponds to the horizontal projection of the rocket flight trajectory. Points and large print indicate the location and names of GPS stations. *T*1 and *T*2 lines are model trajectories of the Transit satellite (at SELE). Thin line (GPS PRN18) shows the trajectory of subionospheric points of intersection of the ionosphere and the CHUM–PRN18 ray path at an altitude of 400 km. Filled squares on the trajectories indicate positions of subionospheric points when TEC disturbances observed at receiving points had maximal amplitudes. Locations of an assumed source of SAW at 100 km altitude are marked by crosses.

wide range of periods. The formation of the extensive network of SRNS receivers, whose data are supplied to the Internet, is also of importance. Thus, the network of GPS receivers network of global navigational system GPS included not less than 900 points in June 2001.

In this work an attempt has been made to analyze the ionospheric response to SAW, generated during rocket launches, using SRNS GPS, as well as to model TEC observations at Transit SRNS. We considered the launches of the Proton and Soyuz carrier rockets performed in 1998–2000 from the Baikonur cosmodrome (44° N, 58° E). Information about launches was obtained from the Internet (http://www.flatoday.com, http://www.spacelaunchesnews.com, and http://www.ilslaunch.com).

Figure 1 shows the experiment geometry during the launches of the Proton carrier rockets from the Baikonur cosmodrome. The symbol ◇ (rhomb) denotes the launch site position. The thick line approximately corresponds to the horizontal projection of the rocket trajectory with an orbital inclination of $\psi = 51.6°$ (http://www.ilslaunch.com). Locations and names of GPS stations are marked by points and capitalized names.

2. REGISTRATION OF A SAW RESPONSE WITH THE HELP OF GPS

In the recent years methods for detecting ionospheric disturbances have been intensely developed based on wide usage of the extensive network of GPS receivers, data from which are accessible via the Internet. We [Afraimovich *et al.*, 1998] have developed the method for determining parameters of wave-like disturbances in the ionosphere (including phase velocity, angular characteristics of a wavevector, direction toward a source, and its position) using phase measurements of TEC $I(t)$ at several spaced two-frequency GPS receivers.

GPS measurements are performed with a high degree of accuracy. Therefore, although the initial magnitude of TEC is unknown, the error in determining relative variations in TEC values averaged over 30 s does not exceed 10^{14} m^{-2} [Hofmann-Wellenhof *et al.*, 1992]. This makes it possible to detect ionization inhomogeneities and wave processes in the ionosphere in the wide range of amplitudes (up to 10^{-4} of the diurnal TEC variation) and periods (from several days to 5 min). Below we will use a TEC unit (TECU) equal to 10^{16} m^{-2}, generally accepted in the literature.

To determine characteristics of waves generated in the ionosphere by a carrier rocket, we select three stations (A, B, and C), the distances between which do not exceed the half of the expected wavelength Λ of a disturbance. Point B is considered as the center of the topocentric frame of reference with the x and y axes pointed to east and north, respectively. Such a configuration of receivers represents the GPS array.

The initial data for calculations include the series of TEC values for three selected points $I_A(t)$, $I_B(t)$, and $I_C(t)$ and the corresponding series of the elevation angle, $\theta_S(t)$, and azimuth, $\alpha_S(t)$, of the beam to the satellite. In this case we select the continuous series of measurements $I_A(t)$, $I_B(t)$, and $I_C(t)$ with a duration of not less than one hour including the time of the rocket launch. To exclude variations in the regular ionosphere, as well as trends caused by the motion of the satellite, we use the procedure of trend removal with a selected time window.

Since the signal-to-noise ratio in our experiments exceeds unity, the horizontal projection of the SAW phase velocity may be determined (at given coordinates of points A, B, and C) from relative time shifts between instants t_p corresponding to the maximal TEC deviation at these points. The magnitude V_h and azimuth α of the SAW wavevector $\mathbf{K_t}$ in the angle range 0°–360° may be calculated using the linear transformation described by Afraimovich *et al.*, [1998].

A few (not less than four) GPS satellites are visible simultaneously at each receiving station. Accordingly, several TEC values may be obtained simultaneously for different lines of sight to satellites **r**. If θ and α are the elevation angle and azimuth of the $\mathbf{K_t}$ vector, then the

angle γ between the direction of propagation of a wave disturbance $\mathbf{K_t}$ and the line of sight ray $\mathbf{r}$ is defined by

$$\cos(\gamma) = \cos(\theta_S)\cos(\theta)\cos(\alpha_S - \alpha) + \sin(\theta_S)\sin(\theta). \quad (1)$$

The maximum amplitude of a TEC disturbance will be observed for those SAW, the wavevector ($\mathbf{K_t}$) of which is perpendicular to the direction of $\mathbf{r}$, i.e., when the condition $\cos(\gamma) = 0$ is satisfied. Or

$$\tan(\theta) = -\cos(\alpha_S - \alpha)/\tan(\theta_S). \quad (2)$$

The aspect condition (2) limits the number of ray paths to a satellite, for which the reliable detection of the SAW response is possible against a noise background. On the other hand, Eq. (2) makes it possible to determine the elevation angle of the shock wavevector $\mathbf{K_t}$ and the magnitude of the phase velocity $V_t = V_h \cos\theta$.

Panels (a) and (d) in Fig. 2 show typical time variations in TEC, $I(t)$, for four GPS satellites (PRN16, PRN18, PRN19, and PRN22) at CHUM station of the GPS array in the region of the Baikonur cosmodrome during the launch of the Proton carrier rocket at 2106 UT on April 17, 2000. The TEC time variations, $dI(t)$, for the same satellites after the trend removal with the 5-min time window are shown in panels (b) and (e).

It is clear from Fig. 2b that, in the case of the PRN18 satellite, the rapid N-form variations with a characteristic period of $T \sim 300$ s, caused by the SAW propagation, may be easily identified against a background of slow TEC variations. The amplitude of fluctuations (on the order of 0.15 TECU) essentially exceeds the intensity of TEC "background" fluctuations. The delay of the SAW response relative to the launch time is 12 min. In the case of the PRN19 satellite, the oscillations do not display any pronounced structure, and their amplitude is significantly less (not more than 0.06 TECU). The TEC disturbances on trajectories of PRN16 and PRN22 ray paths (Fig. 2e) are almost indistinguishable among random noise variations of TEC. The standard deviation of the TEC fluctuations constitutes 0.02 TECU for PRN16 and 0.01 TECU for PRN22, and the amplitude of disturbances near the launch time t_0 does not exceed 0.05 TECU.

The aspect dependence of the TEC amplitude was investigated in detail by Afraimovich *et al.*, [1992; 1998]. It was shown [Afraimovich *et al.*, 1992] that, for the ionization distribution close to Gaussian, the amplitude of TEC disturbances depends on the angle γ and the ratio of a disturbance wavelengths Λ to the half-width of the ionization maximum h_d

$$M(\gamma) \propto \exp\left[-\frac{(\pi h_d \cos(\gamma))^2}{(\Lambda\cos(\theta_S))^2}\right]. \quad (3)$$

To compare the character of the aspect dependence of TEC disturbances recorded during the launch with the theoretical calculations, we modeled wave-like disturbances of the electron density for the observational conditions on April 17, 2000.

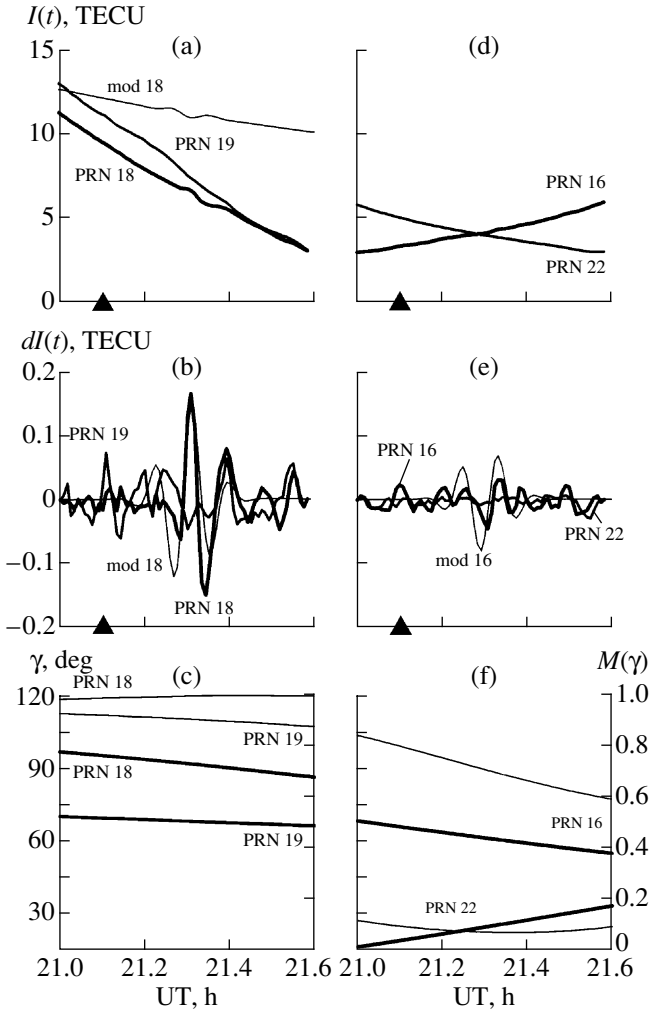

Fig. 2. (a, d) Time variations in TEC, $I(t)$, and (b, e) the $dI(t)$ variations without a trend for four GPS satellites (PRN16, PRN18, PRN19, and PRN22) for CHUM station in the Baikonur cosmodrome region during the launch of the Proton carrier rocket on April 17, 2000. Thick and thin lines show experimental and model data, respectively. Arrows at the abscissa axis indicate the rocket launch instant (t_0). Panels (c) and (f) show the calculated time variations in the angle γ between the propagation direction of the wave disturbance and the line of sight to the satellites (thick lines), as well as the theoretical variations in the TEC response amplitude, $M(\gamma)$, (thin lines).

The model of TEC measurements with the help of the GPS interferometer, developed by us [Afraimovich *et al.*, 1998], makes it possible to calculate the spatial and temporal distribution of the electron density N_e in the ionosphere close to real distribution and then, using coordinates of receiving stations and satellites, to integrate N_e along the receiver–satellite ray path with a given time step. As a result, we obtain the TEC time series similar to the input experimental data $I_A(t)$, $I_B(t)$,

and $I_C(t)$, which may be processed by the same methods as were used for processing the experimental series.

The ionization model takes into account the height distribution of N_e, diurnal and seasonal electron density variations controlled by the solar zenith angle, as well as the irregular N_e disturbances with smaller amplitudes in the form of a discrete superposition of planar traveling waves. In this work we took disturbance in the form of a unit wave packet in order to reach the maximal approximation to real conditions for the carrier rocket launch:

$$N_d(t, r) = A_w \exp\left[-\left(\frac{t - t_{\max}}{t_d}\right)^2\right] \cos\left(\frac{2\pi t}{T_W} - \frac{2\pi r}{L_W}\cos(\gamma)\right). \quad (4)$$

Here A_W, T_W, and L_W, are the amplitude, period and wavelengths of the disturbance wave; $t_{\max}$ is the time of the disturbance maximum; t_d is the halfwidth of the wave packet; and r is the magnitude of the radius-vector of a point on the ray path to the satellite. The disturbance parameters were selected to be close to the values obtained from the PRN18 experimental data with technique described here (Fig. 2b): L_W = 421 km, T_W = 6 min, t_d = 4 min, $t_{\max}$ = 21.3 UT, $\theta = 56°$, and $\alpha = 166°$. The wave amplitude constituted 2% of the N_e magnitude in the ionization maximum.

Some results of modeling are given in Figs. 2a, 2b, and 2e (thin lines). Panel (a) shows temporal variations in $I(t)$ for PRN18. One can see some increase in the discrepancy between the experimental and model values of $I(t)$ with increasing elevation angle of the satellite, i.e., with decreasing distance from the satellite. The model TEC values are overestimated. This is probably related to the roughness of the model, which was not aimed at precise describing spatiotemporal variations in the electron content magnitude. This will not affect subsequent calculations, since the trend is removed from the series and only relative variations $dI(t)$ are considered.

The model TEC variations with the removed trend are shown by thin lines in Fig. 2b for PRN18 and in Fig. 2e for PRN16. The trend was removed from model and experimental data with the 5-min time window. Figure 2 shows that, in case of PRN18, the period, amplitude, and form of the TEC response to the wave disturbance propagation in the ionosphere, defined by Eq. (4), almost coincide with the TEC variations observed in the SAW propagation during the launch on April 17, 2000. For PRN19, PRN16, and PRN22 only amplitudes of the calculated and observed TEC variations are close.

Using Eqs. (1) and (3) and setting $\theta = 56°$ and $\alpha = 166°$, we have calculated the theoretical dependence $M(\gamma)$ for four considered satellites during the launch period on April 17, 2000 (Figs. 2c, 2f, thin lines). Thick lines in the same panels indicate variations in the angle γ between the direction of the wave disturbance propagation and the ray path to the satellites. It is evident that the PRN18 conditions are the most favorable for detecting SAW: γ varies from 98° to 89°, and $M(\gamma)$ is equal to unity during the whole observation period. For PRN19. γ does not exceed 70°, as a result of which, the observed TEC response does not, probably, display such a pronounced N-form variation as in the case of PRN18, in spite of the fact that $M(\gamma)$ reaches 0.9, but the amplitude of the TEC disturbance is still rather high. For PRN22, the conditions for detecting a response are the worst (Fig. 2f). In this case SAW propagates almost along the line of sight ($\gamma \sim 15°$–$30°$ and $M(\gamma) \sim 0.1$); therefore, the amplitude of the TEC response in Fig. 2e is comparable with the noise level.

The distributions of the main SAW parameters obtained in processing the TEC variations during the launches of the Proton and Soyuz rockets from the Baikonur cosmodrome using the method of Afraimovich *et al.* [1998] are shown in Fig. 3. A total of 18 launches for the 1998–2000 period have been processed. To calculate the SAW parameters, we selected such receiver–satellite ray paths for which the recorded amplitude of the TEC response was maximal. It was assumed that for such rays that the aspect relation (2) was satisfied. The amplitude of disturbances and the SAW period (Fig. 3, panels a, b) were determined for each such ray at all GPS stations available in the region of the Baikonur cosmodrome. In calculating characteristics of the velocity and SAW source position (Fig. 3, panels c–h), we composed different GPS arrays of the selected rays. A data correlation for different launches and rays to satellites has shown a sufficient closeness of the calculated SAW parameters regardless of the geomagnetic disturbance level, season, local time, and configuration of the GPS array.

The amplitude of the TEC response (Fig. 3a) varies in the range 0.01–0.5 TECU, which accounts for 0.03–2% of the diurnal TEC variations. The amplitude of more than a half of the recorded responses are less than 0.1 TECU. Such oscillations exceed random noise variations in TEC (the standard deviation of these oscillations for quiet background days is, as a rule, 0.01–0.02 TECU), which makes it possible to reliably determine the horizontal component and azimuth of the SAW propagation velocity. At the same time, the low amplitude of the TEC oscillations indicates that, in these cases, the aspect condition is, nevertheless, insufficiently satisfied and, when calculating the elevation angle and SAW velocity magnitude, we can only roughly estimate these parameters.

The scatter in the period of the recorded TEC variations is negligible (Fig. 3b). The most frequently observed oscillations have characteristic periods of 240 and 300 s. Our measurements of periods and amplitude of the SAW response agree well with results of radio probing the ionosphere by UHF signal from the MARECS B2 geostationary satellite during the

launches of the Space Shuttle carrier rockets on October 18, 1993, and on February 3, 1994 [Li *et al.*, 1994]. They are also close to estimates made during the measurements of the Doppler frequency shift in the HF range during the launches of Space Shuttle launches on February 28, 1990, and on April 28, 1991 [Jacobson and Carlos, 1994], as well as to similar estimates obtained by Nagorsky [1998] on oblique HF radio paths during the launches of the carrier rockets from the Baikonur cosmodrome.

An analysis of the azimuthal distribution (Fig. 3d) shows a clearly defined southeastward motion of SAW (160° ± 20°). This direction almost coincides with the azimuth of the normal α_0 to the projection of the rocket motion at the initial leg of its trajectory on the Earth's surface (thin line in Fig. 3d). If α varies from 0° to 360°, the accuracy of the azimuth determination is 5.5%.

As one would expect, the elevation angle of the SAW wavevector varies in a wider range: from 30° to 75° (Fig. 3c). The mean value of the elevation angle is 49°, and the standard deviation is about 15°, which is equal to the accuracy of its determination (17%) at θ varying from 0° to 90°. The accuracy is not high but is quite acceptable for geophysical measurements. It should also be noted that the suggested method is one of several methods that make it possible to allowing determine the elevation angle and, knowing it, the total vector of the SAW velocity.

According to our data (Fig. 3e), the average magnitude of the horizontal velocity of the SAW propagation varies between 900 and 1800 m/s (the most probable value is 1600 m/s). The phase velocity (V_t) magnitude at the altitude of the ionospheric F_2 region maximum, which makes the main contribution to the TEC variations, is 600–1200 m/s (Fig. 3f). The value of V_t is close to the sound velocity at these altitudes [Li *et al.*, 1994], which indicates that TEC disturbance is of the sonic origin.

According to published data, the SAW propagation velocity varies in the range 600–1700 m/s [Arendt, 1971; Calais and Minster, 1996; Karlov *et al.*, 1980; Noble, 1990]. This is the velocity horizontal component, and it is determined from the ionospheric response delay relative to the launch time and known distance between the launch site and subionospheric point. For comparison, we have made similar calculations and obtained an average velocity (V_a) of about 700 m/s (Fig. 3f, solid line), which is substantially lower than the most probable value of the horizontal component of the SAW velocity determined by the method of Afraimovich *et al.*, [1998]. We relate such discrepancy to the delay Δt_W of the SAW source "switch-on" relative to the launch instant.

If the angular characteristics (θ and α) of the SAW wavevector ($\mathbf{K_t}$) are known, we can estimate the SAW source coordinates as coordinates of the point at which $\mathbf{K_t}$ crosses the horizontal plane at some altitude h_W.

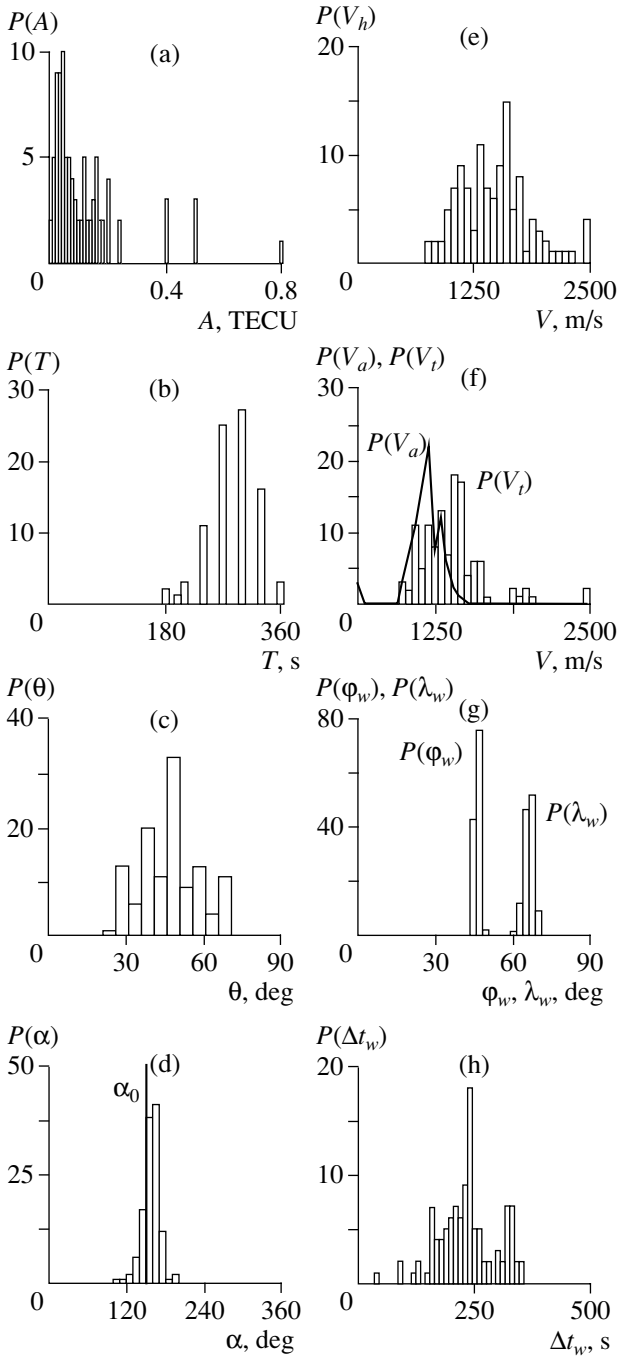

Fig. 3. Distributions of the main parameters of SAW generated during the launches of the Proton and Soyuz rockets from the Baikonur cosmodrome: (a) amplitude of the TEC disturbance; (b) period of SAW; (c, d) the elevation angle θ and azimuth α of the $\mathbf{K_t}$ wavevector, respectively; (e, f) the horizontal component (V_h) and magnitude (V_t) of the SAW phase velocity, respectively; (g) the latitude (φ_W) and longitude (λ_W) of an assumed SAW source at 100 km altitude; (h) the time delay of the "switch-on" of the SAW source relative to the launch instant. The panel (f) shows also the distribution of the mean wave velocity (V_a) computed from the response delay and from the known distance between the launch site and the subionospheric point. The vertical line in the (d) panel indicates the azimuth α_0 of the normal to the initial part of the projection of the rocket trajectory onto the Earth's surface.

Such estimates have been made under the assumption of the rectilinear SAW propagation and neglecting the sphericity. The altitude of the SAW generation h_W was taken equal to 100 km in accordance with [Li *et al.*, 1994; Nagorsky, 1998]. Figures 3g and 3h show results of calculating SAW source coordinates (latitude φ_W and longitude λ_W) and delay Δt_W of the assumed SAW source "switch-on" relative to the carrier rocket launch. In addition, the calculated positions of the source are shown by crosses in Fig. 1. As is seen from this figure, the calculated position of the SAW source during the rocket launches does not coincide with the location of the launch site. At the same time, source coordinates agree rather well with those of the horizontal projection of rocket trajectories. The position of the SAW source corresponds to the trajectory portions at a distance of 700–900 km from the rocket launch site (Fig. 1). The time of the source "switch-on" of the source lags behind the rocket launch time by 200–250 s.

Data obtained agree well with the mechanism substantiated by Calais and Minster [1996], Li *et al.* [1994], and Nagorsky [1998]. These researchers believe that the SAW generation occurs during an almost horizontal active flight at an initial leg of its trajectory at altitudes of the lower atmosphere (100–130 km). A rocket passes along this leg at a supersonic velocity during 100–300 s of flight at a distance of not less than 500 km from a launch site. The SAW source "is switched-on" when a rocket reaches an altitude of about 100 km maintaining its supersonic velocity. Therefore, it is not surprising that the "average" velocity (V_a), usual derived from the response delay relative to the rocket launch, is substantially lower than the phase velocity (V_h).

3. MODELING THE SAW RESPONSE WITH HELP OF TRANSIT SRNS

An attempt has been made to use methods for studying SAW parameters (developed by us for the GPS system [Afraimovich *et al.*, 1998]) to analyze the ionospheric response to the Proton carrier rocket launched on April 17, 2000, based on data of modeling the TEC observations onboard Transit SRNS. Two conditional trajectories (*T*1 and *T*2) of the Transit satellite (Fig. 1) were selected for modeling. During calculations we assumed that the satellite moves in a circular near-polar orbit with a radius of $R_S = R_E + 1000$ km.

As in the case of GPS, the disturbance was specified in the form of a unit wavepacket (4). The values of θ_S and α_S for vector **r** were computed using geographic coordinates of the Transit satellite for given trajectories *T*1 and *T*2. Other initial parameters of a disturbance were selected the same as for GPS: $L_W = 421$ km, $T_W = 6$ min, $t_d = 4$ min, $t_{\max} = 2135$ UT, $\theta = 56°$, and $\alpha = 166°$. The wave amplitude constitutes 2% of the N_e magnitude at the ionization maximum. However, the calculations indicated that the disturbance with such an amplitude have almost no effect on the TEC model variations for Transit satellites. We were forced to increase the wave amplitude up to 10%.

The distance *D* from the satellite (Fig. 4c) was computed by the following formula

$$D^2 = (R_S\cos\varphi_S\cos\lambda_S - R_E\cos\varphi_p\cos\lambda_p)^2 + (R_S\cos\varphi_S\sin\lambda_S - R_E\cos\varphi_p\sin\lambda_p)^2 + (R_S\sin\varphi_S - R_E\sin\varphi_p)^2, \quad (5)$$

where $R_E = 6371$ km is the Earth's radius, $R_S = R_E + 1000$ km is the radius of the Transit satellite orbit, φ_S and λ_S are the satellite geographic latitude and longitude, and φ_p and λ_p are the geographic latitude and longitude of the point of observation.

The $I(t)$ series were processed with by the technique used to process similar data for GPS satellites. To exclude variations in the regular ionosphere and trends due to the satellite motion, we removed trends with a time window of 66 s.

The results of modeling $I(t)$ for trajectory *T*1 are shown in Fig. 4a (line *T*1). The TEC model variations $dI(t)$ with removed trend are given in Fig. 4b (line *T*1). Figures 4a and 4b indicate that an insignificant wave disturbance of the electron density is observed in the $dI(t)$ series near the specified maximum of the wave amplitude at $t_{\max} = 2135$ UT. The amplitude of this disturbance is so small (less than 0.05 TECU) that the wave with given parameters should not perceptibly affect the TEC variations along the considered trajectory of the Transit satellite. This conclusion is also confirmed by an analysis of the aspect conditions for trajectory *T*1. Figure 4d shows variations in the angle γ between the direction of the wave disturbance propagation and the ray path to the Transit satellite (thick line *T*1), as well as the aspect dependence of the TEC amplitude $M(\gamma)$ computed by Eq. (3) (thin line *T*1).

It is clear that, from 2125 to 214 UT, γ does not exceed 60° and $M(\gamma)$ is rather low (0.6–0.2). Thus, the conditions for detecting SAW, caused by the launch of the Proton carrier rocket on the Transit satellite, are very unfavorable. In the case of the GPS system, similar conditions are observed for the PRN16 satellite (Fig. 2f). Accordingly, the amplitude of the TEC response onboard the PRN16 satellite (Fig. 2e) is also comparable with the noise level, which agrees with the model calculations for the GPS system and the Transit SRNS.

Using a mathematical model of visible satellite motion, we can choose such a Transit trajectory that its radius vector would be perpendicular to the SAW wavevector (*T*2 trajectory in Fig. 1). Thereby, the aspect condition (2) will be satisfied and the amplitude of the SAW response will be maximal. We have used such an opportunity. The satellite motion parameters were chosen in such a way that, from 2125 to 2140 UT, the angle between the direction of the wave disturbance propaga-

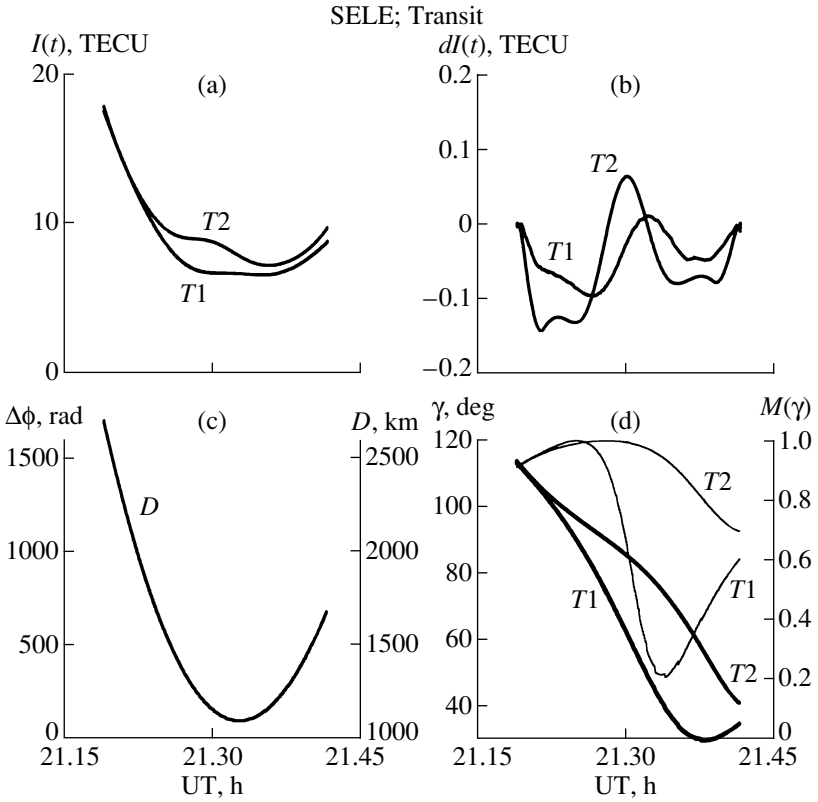

Fig. 4. TEC variations for the *T*1 and *T*2 model trajectories of the Transit satellite computed for SELE during the launch of the Proton rocket on April 17, 2000: (a) time variations in TEC, $I(t)$; (b) $dI(t)$ variations without the trend; (c) the time variations in the distance (D) from the Transit satellite; (d) the time variations in the angle (γ) between the direction of the wave disturbance propagation and the sight of view to the satellites (thick lines), and the theoretical variations in the TEC response amplitude ($M(\gamma)$, thin lines).

tion and the ray path to the satellite would be 90° (thick line *T*2 in Fig. 4d). Figure 4d indicates (thin line *T*2) that the value of the $M(\gamma)$ function is also close to unity during this period. This indicates that the amplitude of the TEC response to the passage of the wave with given parameters should be maximal.

The time variations $I(t)$ obtained for the satellite model trajectory are shown in Fig. 4a by line *T*2. In Fig. 4b the same curve illustrates $dI(t)$ variations whose trend was removed with a time window of 66 s. Indeed, the wave disturbance in the TEC variations is more pronounced. It has the form of an isolated half-wave (wavepacket) with a maximum at 2130 UT and a half-width of about 4 min, i.e., with parameters close to the specified ones. It is interesting to note that the "carrier" component (the wave with a period of 6 min) specified in the wave model is not observed in the TEC variations on the Transit trajectory, although it is evident in the model variations for GPS satellites (thin lines in Figs. 2b, 2e). The amplitude of the $dI(t)$ disturbance is ~0.1 TECU. The oscillations with the same amplitude are also observed also at the GPS system on PRN18 (Fig. 2b), where the conditions for the SAW detection are similar. At the same time, the magnitude and form of the obtained TEC disturbance is in bad agreement with the input parameters of the model.

Thus, data obtained from the model for receiving the signals from the Transit SRNS do not allow us to reliably correlate the recorded wave disturbances in the TEC with SAW caused by rocket launches.

4. CONCLUSIONS

This investigation have revealed a high efficiency of using SRNS GPS for detecting ionospheric responses to SAW generated during launches of carrier rockets. It has been shown that the ionospheric SAW response has the form of wave disturbances with periods of 250–300 s. The methods developed by us have made it possible to calculate not only the azimuth and the horizontal component of the velocity of these WID, but also the elevation angle of the wavevector, magnitude of the phase velocity, and coordinates and time of "switch-on" of the SAW source. A statistical analysis of data, obtained for 18 the Proton and Soyuz carrier rockets launched from the Baikonur cosmodrome in 1998–2000, has revealed the clearly defined south–east direction of the SAW motion (160° ± 20°) coinciding with the azimuth of the normal to the projection of the rocket motion trajectory

on the Earth's surface. The elevation angle of the SAW wavevector varied from 30° to 75°. The phase velocity magnitudes at the height of the ionospheric F_2 region maximum are 600–1200 m/s, which is close to the sound velocity at these altitudes. The calculated position of the SAW source does not coincide with the location of the launch site and is on the horizontal projection of the carrier rocket trajectories. The time of the source "switch-on" lags behind the launch time by 200–250 s. Results obtained agree well with results obtained by other researchers and with the recent knowledge of the mechanisms of SAW generation during launches of heavy-lift vehicles.

The Transit SRNS makes it impossible to reliably detect and determine parameters of short-period wave disturbances of the TEC caused by the SAW by virtue of a high relative velocity of its satellites.

ACKNOWLEDGMENTS

This work was supported by INTAS (grant 99-1186), Leading Scientific Schools of the Russian Federation (grant no. 00-15-98509), and the Russian Foundation for Basic Research (project nos. 99-05-64753, 00-05-72026, 01-05-06171).

REFERENCES

Afraimovich, E.L., Terechov, A.I., Udodov, M.Yu., and Fridman, S.V., Refraction Distortions of Transionospheric Radio Signals Caused by Changes in a Regular Ionosphere and by Travelling Ionospheric Disturbances, *J. Atmos. Solar–Terr. Phys.*, 1992, vol. 54, pp. 1013–1020.

Afraimovich, E.L., Palamartchouk, K.S., and Perevalova, N.P., GPS Radio Interferometry of Travelling Ionospheric Disturbances, *J. Atmos. Solar–Terr. Phys.*, 1998, vol. 60, pp. 1205–1223.

Arendt, P.R., Ionospheric Undulations Following "Appolo-14" Launching, *Nature* (London), 1971, vol. 231, pp. 438–439.

Calais, E. and Minster, J.B., GPS Detection of Ionospheric Perturbations Following a Space Shuttle Ascent, *Geophys. Res. Lett.*, 1996, vol. 23, pp. 1897–1900.

Carlos, R.C. and Massey, R.S., The Los Alamos Beacon Receiver Array, *IEEE Transacrions on Geosciences and Remote Sensing*, 1994, vol. 32, pp. 954–958.

Hofmann-Wellenhof, V., Lichtenegger, H., and Collins, J., *Global Positioning System: Theory and Practice*, New-York: Springer-Verlag, 1992.

Jacobson, A.R. and Carlos, R.C., Observations of Acoustic-Gravity Waves in the Thermosphere Following Space Shuttle Ascents, *J. Atmos. Solar–Terr. Phys.*, 1994, vol. 56, pp. 525–528.

Karlov, V.D., Kozlov, S.I., and Tkachev, G.N., Large-Scale Disturbances in the Ionosphere Originating during an Active Flight, *Kosm. Issled.*, 1980, vol. 18, p. 266.

Li, Y.Q., Jacobson, A.R., Carlos, R.C., Massey, R.S., Taranenko, Y.N., and Wu, G., The Blast Wave of Shuttle Plume at Ionospheric Heights, *Geophys. Res. Lett.*, 1994, vol. 21, pp. 2737–2740.

Nagorskii, P.M., Nonuniform Structure of the Ionospheric *F* Region Formed by Rockets, *Geomagn. Aeron.*, 1998, vol. 38, no. 1, pp. 100–106.

Noble, S.T., A Large-Amplitude Traveling Ionospheric Disturbance Exited by the Space Shuttle during Launch, *J. Geophys. Res.*, 1990, vol. 95, pp. 1937–1944.